The Astrophysical Journal, 594:961–970, 2003 September 10

CONSTRAINING THE EVOLUTION OF ZZ CETI

Anjum S. Mukadam,[1,2] S. O. Kepler,[3,4,5] D. E. Winget,[1,2] R. E. Nather,[1,2] M. Kilic,[1,2] F. Mullally,[1,2] T. von Hippel,[1,2] S. J. Kleinman,[6] A. Nitta,[6] J. A. Guzik,[7] P. A. Bradley,[7] J. Matthews,[8] K. Sekiguchi,[9] D. J. Sullivan,[10] T. Sullivan,[10] R. R. Shobbrook,[11] P. Birch,[12] X. J. Jiang,[13] D. W. Xu,[13] S. Joshi,[14] B. N. Ashoka,[15] P. Ibbetson,[16] E. Leibowitz,[16] E. O. Ofek,[16] E. G. Meištas,[17,18] R. Janulis,[17,18] D. Ališauskas,[18] R. Kalytis,[18] G. Handler,[19] D. Kilkenny,[19] D. O'Donoghue,[19] D. W. Kurtz,[20,21] M. Müller,[22] P. Moskalik,[23] W. Ogłoza,[23,24] S. Zoła,[24,25] J. Krzesiński,[24] F. Johannessen,[26] J. M. Gonzalez-Perez,[26] J.-E. Solheim,[26] R. Silvotti,[27] S. Bernabei,[28] G. Vauclair,[21] N. Dolez,[21] J. N. Fu,[21] M. Chevreton,[29] M. Manteiga,[30] O. Suárez,[30,31] A. Ulla,[31] M. S. Cunha,[32,33] T. S. Metcalfe,[1,34] A. Kanaan,[35] L. Fraga,[35] A. F. M. Costa,[3,4] O. Giovannini,[4,36] G. Fontaine,[37] P. Bergeron,[37] M. S. O'Brien,[38] D. Sanwal,[39] M. A. Wood,[40] T. J. Ahrens,[41] N. Silvestri,[40] E. W. Klumpe,[41] S. D. Kawaler,[42] R. Riddle,[42] M. D. Reed,[43] and T. K. Watson[44]

Received 2003 April 15; accepted 2003 May 19

ABSTRACT

We report our analysis of the stability of pulsation periods in the DAV star (pulsating hydrogen atmosphere white dwarf) ZZ Ceti, also called R548. On the basis of observations that span 31 years, we conclude that the period 213.13 s observed in ZZ Ceti drifts at a rate $dP/dt \leq (5.5 \pm 1.9) \times 10^{-15}$ s s^{-1}, after correcting for proper motion. Our results are consistent with previous $\dot{P}$ values for this mode and an improvement over them because of the larger time base. The characteristic stability timescale implied for the pulsation period is $\mid P/\dot{P} \mid \geq 1.2$ Gyr, comparable to the theoretical cooling timescale for the star. Our current stability limit for

[1] Department of Astronomy, University of Texas at Austin, 1 University Station, C1400, Austin, TX 78712; anjum@astro.as.utexas.edu.
[2] McDonald Observatory, Fort Davis, TX 79734.
[3] Instituto de Física, Universidade Federal do Rio Grande do Sul, 91501-970 Porto Alegre, RS Brazil.
[4] Visiting Astronomer, Laboratório Nacional de Astrofísica, operated by the Ministério de Ciência e Tecnologia, Brazil.
[5] Visiting Astronomer, Cerro Tololo Inter-American Observatory, operated by AURA for the NSF.
[6] Apache Point Observatory, P. O. Box 59, Sunspot, NM 88349.
[7] Los Alamos National Laboratory, X-2, MS B220, Los Alamos, NM 87545-2345.
[8] Department of Physics and Astronomy, University of British Columbia, Vancouver, BC V6T 1Z4, Canada.
[9] Subaru Telescope, National Astronomical Observatory of Japan, 650 North A'ohoku Place, Hilo, Hawaii 96720.
[10] School of Chemical and Physical Sciences, Victoria University of Wellington, P.O. Box 600, Wellington, New Zealand.
[11] Research School of Astronomy and Astrophysics, Australian National University, Weston Creek PO, ACT 2611, Australia.
[12] Perth Observatory, Walnut Road, Bickley, Western Australia 6076, Australia.
[13] Beijing Astronomical Observatory and Joint Laboratories of Optical Astronomy, National Astronomical Observatories of China, Beijing 100012, China.
[14] Uttar Pradesh State Observatory, Manora Peak, 263 129 Nainital, India.
[15] Indian Space Research Organization, Technical Physics Division, ISRO Satellite Center, Airport Road, Bangalore 560 017, India.
[16] School of Physics and Astronomy and the Wise Observatory, Tel Aviv University, Ramat Aviv, Tel Aviv 69978, Israel.
[17] Institute of Theoretical Physics and Astronomy, Goštauto 12, Vilnius 2600, Lithuania.
[18] Vilnius University Observatory, Čiurlionio 29, Vilnius 2009, Lithuania.
[19] South African Astronomical Observatory, P.O. Box 9, Observatory 7935, South Africa.
[20] Centre for Astrophysics, University of Central Lancashire, Preston, PR1 2HE, UK.
[21] Observatoire Midi-Pyrenees, 14 Avenue E. Belin, 31400 Toulouse, France.
[22] Department of Astronomy, University of Cape Town, Rondebosch 7701, South Africa.
[23] N. Copernicus Astronomical Center, Polish Academy of Sciences, ul. Bartycka 18, 00-716 Warsaw, Poland.
[24] Mount Suhora Observatory, Cracow Pedagogical University, ul. Podchorych 2, 30-084 Cracow, Poland.
[25] Astronomical Observatory, Jagiellonian University, ul. Orla 171, 30-244 Krakow, Poland.
[26] Institutt for Fysikk, Universitetet i Tromsø, N-9037 Tromsø, Norway.
[27] Instituto Nazionale di AstroFisica-Osservatorio Astronomico di Capodimonte, via Moiariello 16, I-80131 Naples, Italy.
[28] Instituto Nazionale di AstroFisica-Osservatorio Astronomico di Bologna, via Ranzani 1, I-40127 Bologna, Italy.
[29] Observatoire de Paris Meudon, 92195 Meudon, France.
[30] Universidade da Coruña, Departamento de Ciencias Naúticas e da Terra, Spain.
[31] Universidade de Vigo, Departamento de Física Aplicada, Spain.
[32] Centro de Astrofisica da Universidade do Porto, Rua das Estrelas, 4150 Porto, Portugal.
[33] Instituto Superior da Maia, Av. Carlos Oliveira Campos, Castelo da Maia, 4475-690 Avioso S. Pedro, Portugal.
[34] Harvard-Smithsonian Center for Astrophysics, 60 Garden Street, Cambridge, MA 02138.
[35] Departamento de Fisica, Universidade Federal de Santa Catarina, 88040-900 Florianopolis, SC Brazil.
[36] Departamento de Fisica e Quimica, Universidade de Caxias do Sul, 95001-970 Caxias do Sul, RS Brazil.
[37] Département de Physique, Université de Montréal, P.O. Box 6128, Station Centreville, Montréal, QC H3C 3J7, Canada.
[38] Space Telescope Science Institute, 3700 San Martin Drive, Baltimore, MD 21218.
[39] Department of Astronomy and Astrophysics, Pennsylvania State University, University Park, PA 16802.
[40] Department of Physics and Space Sciences and SARA Observatory, Florida Institute of Technology, 150 West University Boulevard, Melbourne, FL 32901-6975.
[41] Department of Physics and Astronomy, Middle Tennessee State University, Murfreesboro, TN 37132.
[42] Department of Physics and Astronomy, Iowa State University, Ames, IA 50011.
[43] Southwest Missouri State University, 901 South National, Springfield, MO 65807.
[44] Information Technology Services, Southwestern University, Georgetown, TX 78626.

the period 213.13 s is only slightly less than the present measurement for another DAV, G117-B15A, for the period 215.2 s, establishing this mode in ZZ Ceti as the second most stable optical clock known, comparable to atomic clocks and more stable than most pulsars. Constraining the cooling rate of ZZ Ceti aids theoretical evolutionary models and white dwarf cosmochronology. The drift rate of this clock is small enough that we can set interesting limits on reflex motion due to planetary companions.

Subject headings: stars: evolution — stars: individual (ZZ Ceti, R548) — stars: oscillations — stars: variables: other — white dwarfs

1. INTRODUCTION

Global pulsations of stars can be used to probe their interiors, similar to the method of using earthquakes to explore the Earth's interior. This technique, called asteroseismology, is a unique method to study stellar interiors.

The observed properties of the currently known classes of pulsating white dwarfs place them in three different temperature ranges: the high-temperature instability strip consists of the PNNV (planetary nebula nuclei variable) and the DOV (hot degenerate variable; GW Vir) stars at an effective temperature of 80,000–170,000 K and $\log g \approx 6$; the DBV (helium atmosphere variable) instability strip occurs around 25,000 K, $\log g \approx 8$; while the DAV (hydrogen atmosphere variable) instability strip is found between 11,000 and 12,500 K, $\log g \approx 8$ (see the review paper Winget 1998 and the references therein). The DAV white dwarf stars are also known as the ZZ Ceti stars after ZZ Ceti (R548), the prototype of the class. Their pulsation periods are typically 100–1200 s, consistent with nonradial g-mode pulsations. Pulsating DA white dwarfs (DAVs) are not unusual or special in any way; all known DAs pulsate when their temperatures reach the DAV instability strip (Robinson 1979; Fontaine et al. 1985); i.e., pulsation is an evolutionary phase.

There are two competing internal evolutionary processes that govern the change in pulsation period with time ($\dot{P}$) for a single mode in the theoretical models of the ZZ Ceti stars. Cooling of the star increases the period as a result of the increasing degeneracy, and residual gravitational contraction decreases the period (Winget, Hansen, & Van Horn 1983). For high effective temperatures, as in the DOV/PNNV instability strip, contraction is still significant. Kepler et al. (2000) conclude that the evolutionary $\dot{P}$ is dictated by the rate of cooling for the DAV stars, and contraction is not significant in the temperature range of the DAV instability strip.

The cooler DAV stars exhibit many pulsation modes, the amplitudes of which are observed to change significantly on timescales that are orders of magnitude shorter than the evolutionary cooling (Kleinman et al. 1998). Near the high-temperature (blue) edge of the DA instability strip, we observe the pulsation periods and amplitudes to be highly stable. This implies that a hot DAV star should show a $\dot{P}$ reflective of its cooling rate. G117-B15A is a hot DAV star with a constraining limit $\dot{P} \leq (2.3 \pm 1.4) \times 10^{-15}$ s s^{-1} for the 215.1973907 s period (Kepler et al. 2000). We define a stability timescale $\tau_s \equiv | P/\dot{P} |$; it is the time taken by a clock to lose or gain a cycle. G117-B15A is the most stable optical clock known, with $\tau_s \geq 3.0$ Gyr.

When we measure the cooling rate of a DAV, it applies to all white dwarfs of that temperature, mass, and chemical composition, as pulsation is only a phase in the life of the star. By measuring the cooling rate of another hot DAV such as ZZ Ceti, we are providing a second independent measurement of the cooling rate of a 12,000 K white dwarf. A second measurement is important to apply the results to DA white dwarfs as a class; the DAs constitute 80% of the white dwarf population.

Monitoring the stable hot DAV stars has at least two interesting applications (see § 8). White dwarf evolution is dominated by cooling, leading to a simple relation between effective temperature and age of the white dwarf, described approximately by Mestel cooling theory (Mestel 1952; Van Horn 1971). Measuring the cooling rates of white dwarfs proves helpful in calibrating the white dwarf cooling curve. This reduces some of the theoretical uncertainty in white dwarf cosmochronometry (e.g., Winget et al. 1987; Hansen et al. 2002). Second, stable clocks with an orbital planet will show a detectable reflex motion around the center of mass of the system, providing a means to detect the planet (Kepler et al. 1990, 1991; Mukadam, Winget, & Kepler 2001). Theoretical work indicates outer terrestrial planets and gas giants will survive (e.g., Vassiliadis & Wood 1993) and be stable on timescales longer than the white dwarf cooling time (Duncan & Lissauer 1998). The success of a planet search with this technique around stable pulsators relies on finding and monitoring a statistically significant number of hot DAV stars.

Using standard evolutionary theory, Bradley, Winget, & Wood (1992) estimated the cooling timescale, i.e., $T/\dot{T}$, for a hot DAV at about 12,000 K to be a few billion years. We thus expect the pulsational stability timescale ($P/\dot{P}$) to be a few billion years, which implies that we need decades of data to get a detectable change in period. G117-B15A, ZZ Ceti (R548), L19-2, and G226-29 are four hot DAV stars with suitable time spans of archival data, and we intend to monitor all of them. In this paper, we present our work on ZZ Ceti.

2. OBSERVATIONS

We obtained time series photometry data on ZZ Ceti from 1970 to 1993, most of which were acquired with phototubes. We also have data from the 3.6 m Canada-France-Hawaii Telescope (CFHT), acquired in 1991. Additionally, ZZ Ceti was included as a secondary target star in the Whole Earth Telescope (WET; Nather et al. 1990) campaign XCov 18 in 1999 November and XCov 20 in 2000 November.

We observed ZZ Ceti extensively on the 0.9 and 2.1 m telescopes at McDonald Observatory in 1999 and 2000 with P3Mudgee, a three-star photometer (Kleinman, Nather, & Phillips 1996). In 2001 November, we also acquired high signal-to-noise data by using our new prime-focus CCD photometer, Argos, at the 2.1 m telescope (Nather & Mukadam 2003). This instrument on the 2.1 m telescope has an efficiency equivalent to P3Mudgee on a 6 m telescope. Our observations extend the time base on ZZ Ceti by 8 years, increasing it to a total time span of 31 years. Our

TABLE 1
DOMINANT MODES IN ZZ CETI (R548)

Period (s)	Amplitude (mma)[a]
213.1326.....	6.7
212.7684.....	4.1
274.2508.....	4.1
274.7745.....	2.9

[a] One millimodulation amplitude (mma) equals 0.1% change in intensity.

journal of observations for all the data from 1999 to 2001 is published in Table 1 of Mukadam et al. (2003).

The dominant power in the pulsational spectrum of ZZ Ceti resides in two doublets at 213 and 274 s (Stover et al. 1980; Tomaney 1987) with a spacing of 0.5 s (see Table 1). In our experience, better timing is obtained for as small an integration time as is feasible; we found an integration time of 5 s to be ideal for P3Mudgee on the 0.9 m telescope, and 3 s for Argos on the 2.1 m telescope at McDonald Observatory. This sets the Nyquist frequency at 0.1 Hz, well beyond the range of the observed pulsation spectrum (Kepler et al. 1982). We did not use a filter with the blue-sensitive three-star photometer to maximize the signal-to-noise ratio; we used a BG 40 Schott glass filter with Argos.[45] This does not constitute a problem as the nonradial g-mode pulsations have the same phase in all colors (Robinson, Kepler, & Nather 1982; Nitta et al. 1999).

3. DATA REDUCTION

We reduced and analyzed the data in a manner described by Nather et al. (1990) and Kepler (1993), correcting for extinction and sky variations. After this preliminary reduction, we brought the data to the same fractional amplitude scale and converted the times of arrival of photons to barycentric coordinated time (TCB; Standish 1998). We computed a Fourier transform (FT) for all the data sets. Figure 1 shows our best FT from multisite and extensive single-site observations of ZZ Ceti in 1999.

4. DATA ANALYSIS

Before a $\dot{P}$ measurement can prove meaningful toward determining a cooling rate, we require that the dominant modes in the star do not strongly interact with each other, have stable amplitudes, and are well resolved in the data. We make a critical assumption: we assume that the star does the same thing when we are not looking as when we are.

We used three different techniques to determine $\dot{P}$: direct method, $O-C$ diagram, and the direct nonlinear least-squares approach. The doublets were clearly resolved in seasonal observations in the years 1970, 1975, 1980, 1986, 1991, 1993, 1999, and 2000; they are just barely resolved in 2001. The 1991 data set spans only 5 days and is our shortest season. Most seasons span over a month, and hence their phases are more reliable. We used only the above listed seasons from all our data spanning 1970–2001 for the direct method (§ 4.1) and the $O-C$ diagram (§ 4.2). We were able to utilize all our data for the nonlinear least-squares technique (§ 4.3).

[45] Amplitudes can be underestimated by as much as 20% for a DAV (Kanaan et al. 2000) if we use a red-sensitive photo tube or a CCD to acquire the data. We have to use a filter (e.g., BG 18, BG 38, BG 39, or BG 40 glass) with red-sensitive detectors to suppress the red part of the spectrum and to measure amplitudes reliably. This reduces the photon count but yields amplitudes comparable to blue-sensitive bi-alkali photomultipliers.

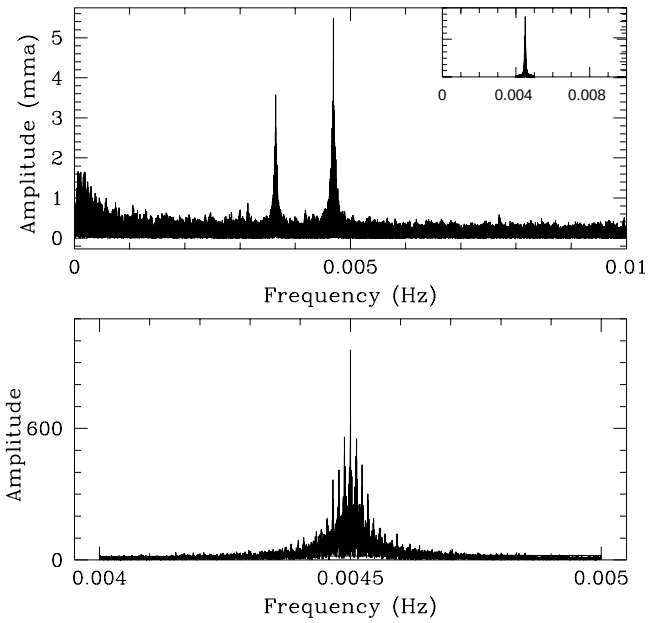

FIG. 1.—*Top*, Fourier transform (FT) of the data on ZZ Ceti from 1999; *bottom*, window pattern, what a single frequency in that data set should look like on an expanded scale; *top inset*, window pattern at the same scale as the FT.

4.1. *Direct Method*

The brute-force direct method consists of plotting the best period for each individual season versus time and equating the best-fit slope to a constraint on the value of $\dot{P}$, as shown in Figures 2 and 3. To obtain these seasonal values, we fit both periods of the doublets simultaneously using a nonlinear least-squares program. The true uncertainties in these values are larger than the formal nonlinear least-squares uncertainties due to pattern and alias noise. Alias noise is caused by the finite extent of the data and the gaps in them and is non-Gaussian in nature. Alias noise can be reduced by multisite observations using instruments such as the WET, which consists of a collaboration of observatories around the globe, and can observe a given pulsator for 24 hr per day. Pattern noise has an underlying structure and is also non-Gaussian (Schwarzenberg-Czerny 1991, 1999). The two frequencies in the doublets are closely spaced; one frequency represents a source of non-Gaussian noise while determining the phase, period, and amplitude for the other. We can decrease pattern noise by increasing the time span of observations, thereby better resolving the doublets.

Our best seasonal periods are shown in Tables 2 and 3, along with their uncertainties. Our linear least-squares fit, shown in the plot in Figure 2, yields $\dot{P} = (0.5 \pm 2.4) \times 10^{-13}$ s s^{-1} for $P_0 = 213.13245 \pm 0.00009$ s and $\dot{P} = (10 \pm 10) \times 10^{-13}$ s s^{-1} for $P_0 = 212.7694 \pm 0.0004$ s. Figure 3 shows a plot of the best periods for the 274 s doublet versus

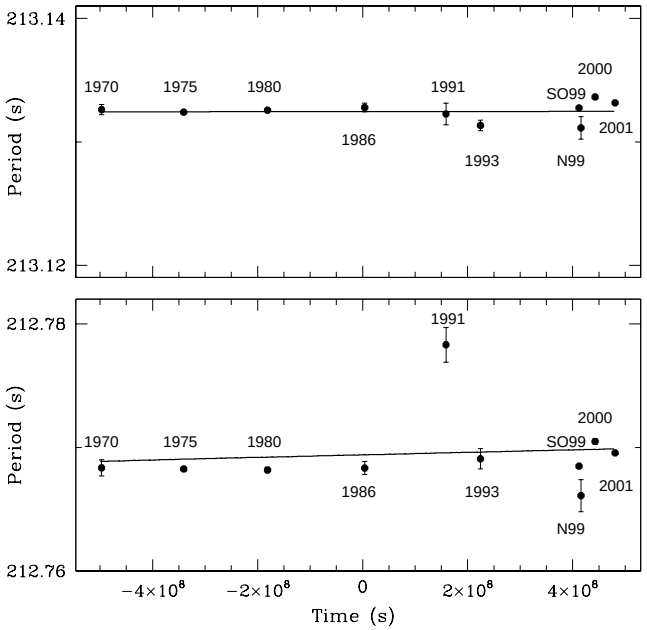

FIG. 2.—Direct method: best seasonal periods vs. time for the 213 s doublet, useful in ruling out large values of $\dot{P}$. *Top*, Best-fit $\dot{P} = (0.5 \pm 2.4) \times 10^{-13}$ s s^{-1} for $P_0 = 213.13245 \pm 0.00009$ s; *bottom*, best-fit $\dot{P} = (10 \pm 10) \times 10^{-13}$ s s^{-1} for $P_0 = 212.7694 \pm 0.0004$ s. The 1991 data set spans over 5 days and contains only 21 hr of data, while other seasons span over a month on average.

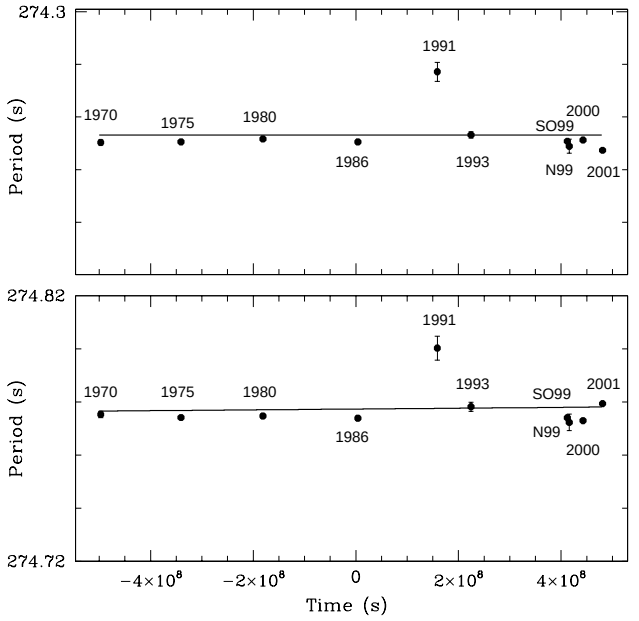

FIG. 3.—Direct method: best seasonal periods vs. time for the 274 s doublet. *Top*, Best-fit $\dot{P} = (-0.4 \pm 27) \times 10^{-13}$ s s^{-1} for $P_0 = 274.253 \pm 0.001$ s; *bottom*, best-fit $\dot{P} = (16 \pm 26) \times 10^{-13}$ s s^{-1} for $P_0 = 274.7774 \pm 0.0009$ s.

TABLE 2
$O - C$ VALUES

$O - C$ (s)	Error in $O - C$ (s)	Epoch	Season	Period (s)
1.4	3.7	−2,346,428	1970	213.13261 ± 0.00041
0.4	1.6	−1,617,531	1975	213.132403 ± 0.000093
1.0	2.4	−862,740	1980	213.13256 ± 0.00014
0.0	2.8	0	1986	213.13277 ± 0.00035
8.3	1.2	743,874	1991	213.13226 ± 0.00087
3.7	1.0	1,049,404	1993	213.13132 ± 0.00042
8.3	1.2	1,924,342	1999 Sep–Oct	213.13275 ± 0.00011
7.2	1.5	1,949,381	1999 Nov	213.13112 ± 0.00091
8.9	1.3	2,067,847	2000	213.13363 ± 0.00017
11.0	2.3	2,248,169	2001	213.133141 ± 0.000071

NOTE.—For period $P = 213.13260456 \pm 0.00000041$ s and $\dot{P} \leq (6.1 \pm 3.1) \times 10^{-15}$ s s^{-1}.

TABLE 3
$O - C$ VALUES

$O - C$ (s)	Error in $O - C$ (s)	Epoch	Season	Period (s)
−0.2	5.8	−2,350,444	1970	212.76835 ± 0.00066
3.5	2.6	−1,620,300	1975	212.76826 ± 0.00015
2.7	3.7	−864,217	1980	212.76817 ± 0.00022
0.0	4.2	0	1986	212.76833 ± 0.00054
2.2	1.8	745,148	1991	212.7783 ± 0.0014
−0.9	1.7	1,051,200	1993	212.76907 ± 0.00082
2.1	1.6	1,927,636	1999 Sep–Oct	212.76849 ± 0.00015
1.5	2.0	1,952,718	1999 Nov	212.7661 ± 0.0013
−1.6	1.7	2,071,386	2000	212.77047 ± 0.00025
5.8	2.3	2,252,017	2001	212.769556 ± 0.000068

NOTE.—For period $P = 212.76842927 \pm 0.00000051$ s and $\dot{P} \leq (1.2 \pm 4.0) \times 10^{-15}$ s s^{-1}.

time. We obtain $\dot{P} = (-0.4 \pm 27) \times 10^{-13}$ s s^{-1} for $P_0 = 274.253 \pm 0.001$ s and $\dot{P} = (16 \pm 26) \times 10^{-13}$ s s^{-1} for $P_0 = 274.7774 \pm 0.0009$ s.

This brute-force technique is not very sensitive to determine $\dot{P}$, but it is absolutely essential in ruling out incorrect solutions that may seem just as likely from the more sensitive techniques, the $O-C$ diagram and the direct nonlinear least-squares approach. Both these techniques suffer from cycle count errors between data sets (explained in the next subsection), while the direct method is independent of this error. The uncertainties in the $\dot{P}$ values we obtained for both the doublets prove to be constructive limits in ruling out large changes in period over time.

4.2. *O−C Technique*

The $O-C$ technique (e.g., Kepler et al. 1991) can be used to improve the period estimates for any periodic phenomenon. The O stands for the observed value of the time of maximum (or time of zero) for a cycle or an epoch E that occurs in a data set. The C stands for its calculated value or ephemeris. If $O-C$ values show a linear trend, then the slope indicates a correction to the period. On the other hand, a nonlinear trend in the $O-C$ diagram shows that the period is changing.

We use bootstrapping (Winget et al. 1985) to improve the period and to extend our phase baseline from one observing season to the next available one. Bootstrapping assumes that we know the period precisely enough to predict the phase for the next data set without cycle count ambiguities. As we know that the uncertainties in phase from the least-squares program are underestimated (Winget et al. 1985; Costa, Kepler, & Winget 1999; Mukadam 2000), we checked for cycle errors up to $E \pm 2$. Larger cycle count errors are ruled out by limits from the direct method.

4.2.1. *Results from the O−C Technique*

Our $O-C$ values for the 213 s doublet are plotted in Figure 4 and presented in Tables 2 and 3, along with the best period and $\dot{P}$ values. The zero epoch corresponds to a reference time of maximum (E_0) of 2,446,679.833986 TCB. We obtain $\dot{P} \leq (6.1 \pm 3.1) \times 10^{-15}$ s s^{-1} for the period $P = 213.13260456 \pm 0.00000041$ s. We also found $\dot{P} \leq (1.2 \pm 4.0) \times 10^{-15}$ s s^{-1} for the period $P = 212.76842927 \pm 0.00000051$ s. The $\dot{P}$ values are comparable to their uncertainties and should be thought of as upper limits only. The $\dot{P}$ values for both modes of the 213 s doublet are consistent with $\dot{P}$ measurements for G117-B15A and detailed theoretical evolutionary models. We conclude that these values constrain the evolution of ZZ Ceti.

The $O-C$ diagram for the 274 s doublet shows changes on a timescale that is 100 times faster than the 213 s doublet. This makes the same gaps between data sets too large to determine the cycle counts. As we have already constrained the cooling rate with the 213 s doublet, we can conclude that the $O-C$ diagrams for both modes of the 274 s doublet are not indicative of cooling. Possible short-term variations in phase on the order of a few months to a few years could be swamping out the parabolic effect of the cooling. These modes may be subject to other effects, such as trapping and avoided crossings (Wood & Winget 1988; Brassard et al. 1992; Montgomery 1998; Benvenuto et al. 2002), discussed in § 6.2. Mukadam (2000) contains a table of $O-C$ values for the 274 s doublet.

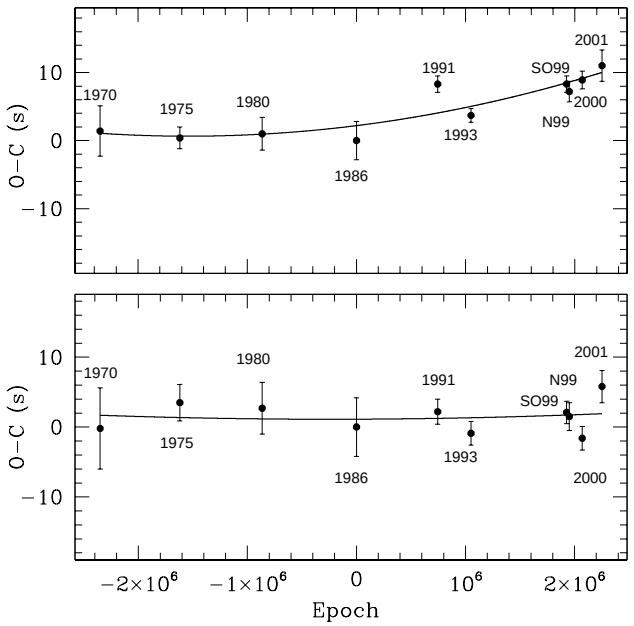

FIG. 4.—*Top*, $O-C$ plot for the 213.13260456 s period, with the best-fit parabola $\dot{P} \leq (6.1 \pm 3.1) \times 10^{-15}$ s s^{-1} drawn as a continuous line; *bottom*, $O-C$ diagram for the period 212.76842927 s with the best fit of $\dot{P} \leq (1.2 \pm 4.0) \times 10^{-15}$ s s^{-1}. The 1991 data set spans only 5 days and is our shortest season. Most seasons span over a month, and hence their phases are more reliable.

4.3. *Direct Nonlinear Least-Squares Fit*

We can fit a variable period to all the data from 1970 to 2001 by using a nonlinear least-squares program to obtain a reliable $\dot{P}$. We fit both periods of the doublet simultaneously to all the data from 1970 to 2001. The program utilizes period, phase, amplitude, and a guess value for $\dot{P}$ as inputs. We fix the amplitude for both periods, optimizing the remaining parameters to minimize the residuals, obtaining a reliable $\dot{P}$ value based on all the data points from 1970 up to 2001. An advantage of this technique over the $O-C$ method is that we can now include all the data in a combined light curve, whether or not the doublets are resolved in individual seasons. These techniques are not completely independent. This technique also suffers from cycle count errors in gaps between data sets, just like the $O-C$ method; when we input a guess value for $\dot{P}$ along with a period, we are effectively feeding in cycle counts for the various epochs; the same bootstrapping process is implicitly applied here.

We obtain $\dot{P} \leq (7.7 \pm 1.9) \times 10^{-15}$ s s^{-1} for $P = 213.132605 \pm 0.000001$ s and $\dot{P} \leq (2.9 \pm 2.8) \times 10^{-15}$ s s^{-1} for $P = 212.768429 \pm 0.000001$ s. The results for the nonlinear least-squares fit are clearly consistent with the $O-C$ technique for both periods within their uncertainties. We do not claim either of these values to be measurements because we have seen them fluctuate with the addition of subsequent seasons; they are not yet reliable as measurements, but they are useful and reliable as constraints.

5. BEST VALUE OF $\dot{P}$ FOR ZZ CETI

We used the $\dot{P}$ limits from the direct method to rule out large changes in the period with time for both doublets. We conclude from the results of the more sensitive techniques, the $O-C$ diagram and the nonlinear least-squares

approach, that the $\dot{P}$ values for the 213 s doublet reflect cooling of the star, while the values for the 274 s doublet do not. This is because evolutionary cooling is expected to be one of the slowest changes, and the 274 s doublet seems to evolve at least 100 times faster than the 213 s doublet. For the context of this paper, we will henceforth discuss only the 213 s doublet as we had set out to measure the cooling rate of the star.

The uncertainties in $\dot{P}$ for both the $O-C$ technique and the nonlinear least-squares method decrease as time-square goes by. The $O-C$ technique uses the seasonal data to obtain the best value for the first time of maximum. These well-determined values then contribute toward finding the optimal solution for $\dot{P}$. The nonlinear least-squares technique utilizes all the points in a data set and therefore directly incorporates all the times of maxima. This increases the reliability of the $\dot{P}$ value; hence, we quote the nonlinear least-squares fits as our best values for the 213 s doublet: $\dot{P} \leq (7.7 \pm 1.9) \times 10^{-15}$ s s^{-1} for $P = 213.132605$ s and $\dot{P} \leq (2.9 \pm 2.8) \times 10^{-15}$ s s^{-1} for $P = 212.768429$ s. The 213.132605 s period has an amplitude of about 6.2 millimodulation amplitude (mma), while the 212.768429 s period is about 4.1 millimodulation mma. The smaller uncertainty in the $\dot{P}$ measurement for $P = 213.132605$ s is clearly a manifestation of larger amplitude and consequently better signal-to-noise ratio, as compared with $P = 212.768429$ s. Therefore the value of $(7.7 \pm 1.9) \times 10^{-15}$ s s^{-1} better reflects the constraining upper limit on $\dot{P}$ for ZZ Ceti.

Tomaney (1987) published his best value, $\dot{P} < (0.4 \pm 9.6) \times 10^{-15}$ s s^{-1}, for the 213 s doublet. This implies that at the 3 σ level his upper limit for the rate of cooling was effectively 29.2×10^{-15} s s^{-1}. Our results are a further refinement due to the larger time base, and they are consistent with previous results.

We claim $\dot{P} \leq (7.7 \pm 1.9) \times 10^{-15}$ s s^{-1} as an upper limit and not as a true measurement. We found fluctuations in the $\dot{P}$ value as we added various seasons of observation, but the uncertainty in $\dot{P}$ always monotonically decreased. This is true for G117-B15A as well and is clearly indicated in Table 1 from Kepler et al. (2000). This leads us to conclude that the uncertainties are true indicators of reliability and are currently more significant than the $\dot{P}$ values. If we determine consistent $\dot{P}$ values for at least three consecutive seasons, then we will believe that it is a measurement and not a constraint. As the $\dot{P}$ for $P = 213.132605$ s is an upper limit, we can conclude that $\dot{P} \leq (2.9 \pm 2.8) \times 10^{-15}$ s s^{-1} for $P = 212.768429$ s is consistent with it. In all subsequent considerations, we will use as our best value $\dot{P} \leq (7.7 \pm 1.9) \times 10^{-15}$ s s^{-1}.

5.1. *Correction Due to Proper Motion*

Pulsating white dwarfs have a nonevolutionary secular period change due to proper motion. Pajdosz (1995) estimated the size of this effect to be on the order of 10^{-15} s s^{-1}. This proper-motion correction to $\dot{P}$ is insignificant for the DOV and PNNV stars because their evolutionary $\dot{P}$ is several orders of magnitude larger. However, it is of the same order as the $\dot{P}$ measured for hot DAVs such as ZZ Ceti and G117-B15A. Pajdosz (1995) demonstrates that the correction is always positive and must be subtracted from $\dot{P}_{\rm obs}$. Using $\mu = 0\farcs236$ yr^{-1} and $\pi = 0\farcs013$ (Harrington & Dahn 1980), we evaluate $\dot{P}_{\rm pm}$ for the four periods along with their respective uncertainties, both of which have been indicated in Table 4. Subtracting out $\dot{P}_{\rm pm}$, we have the following best limit: $\dot{P}_{\rm cool} \leq (5.5 \pm 1.9) \times 10^{-15}$ s s^{-1} for ZZ Ceti.

TABLE 4
Correction in $\dot{P}$ Due to Proper Motion

Period (s)	$\dot{P}_{\rm pm}$ (10^{-15} s s^{-1})	$\sigma_{\dot{P}_{\rm pm}}$ (10^{-15} s s^{-1})
213.132605	2.22	0.36
212.768429	2.22	0.36
274.250804	2.86	0.46
274.774501	2.86	0.46

6. INTERPRETATION OF THE RESULTS

6.1. *Stability of the* 213 s *Doublet*

Using our best limit for the 213 s doublet, $\dot{P} \leq (5.5 \pm 1.9) \times 10^{-15}$ s s^{-1}, we calculate the evolutionary timescale $|P/\dot{P}| \geq 1.2$ Gyr. We compute $\tau_s \geq 0.9$ Gyr and $\tau_s \geq 0.6$ Gyr at the 1 σ and 3 σ levels, respectively.[46] Theoretical models suggest that the 213 s doublet in ZZ Ceti should show a $\dot{P}$ value in the range (2–6) $\times 10^{-15}$ s s^{-1} (e.g., Bradley et al. 1992; Bradley 1996). Our limit is consistent with theoretical calculations of cooling, as well as the $\dot{P}$ measurement for G117-B15A, and is already a constraint on stellar evolution.

The hot DAV stars, which include ZZ Ceti, are expected to exhibit extreme frequency stability, making them reliable clocks. We found this to be true for the 213 s doublet. Theory tells us that this frequency stability may be associated with two different effects: low radial overtone (k) modes and mode trapping. Low k-modes sample the deep interior and have a rate of period change that reflects the global cooling timescale alone. High k-modes have regions of period formation farther out in the star and so may be more easily affected by magnetic fields, rotation, convection, and nonlinear interactions. ZZ Ceti has a measured magnetic field upper limit of about 20 kG (Schmidt & Grauer 1997).

Compositional stratification occurs in white dwarf stars because of gravitational settling and prior nuclear shell burning. A mechanical resonance is induced between the local g-mode oscillation wavelength and the thickness of one of the compositional layers (Winget, Van Horn, & Hansen 1981). This mechanical resonance serves as a stabilizing mechanism in model calculations. For a mode to be trapped in the outer H layer, it needs to have a resonance with the He/H transition region such that its vertical and horizontal displacements both have a node near this interface (Brassard et al. 1992; Montgomery 1998). Note that the H/He interface can also lead to confinement or trapping of modes in the core. Trapped modes are energetically favored, as the amplitudes of their eigenfunctions below the H/He interface are smaller than untrapped modes. Modes trapped in the envelope can have kinetic oscillation energies lower by a few orders of magnitude, compared with the adjacent

[46] To calculate these limits, we cannot use the differential approach as the uncertainties in $\dot{P}$ are comparable to the value itself. We calculate a 1 σ limit from the expression $P/(|\dot{P}| + \sigma_{\dot{P}})$ and a 3 σ limit from $P/(|\dot{P}| + 3\sigma_{\dot{P}})$.

nontrapped modes (Winget et al. 1981; Brassard et al. 1992). Benvenuto et al. (2002) claim a marked weakening of mode-trapping effects with a time-dependent element diffusion in the DA white dwarf models with different thicknesses of the hydrogen envelope.

The resonance condition changes as the star cools, and this can lead to an avoided crossing, as explained in § 6.2. As a DAV cools within the instability strip, trapped modes spend about a quarter of their time in an avoided crossing, during which they are expected to indicate a larger $\dot{P}$ than due to cooling. The trapped modes are stable only for three quarters of the total time spent in the instability strip, when they are not undergoing an avoided crossing. During that time, they evolve more slowly than untrapped modes by a factor ≥ 2 (Bradley et al. 1992; Bradley 1993). Modes of differing k sample slightly different regions in the star with correspondingly different evolutionary timescales; hence, we expect each mode to have a slightly different rate of period change (Wood & Winget 1988).

All the hot DAV stars known are low k-pulsators, including ZZ Ceti. Bradley (1998) identified the 213 s doublet as $l = 1$, $k = 2$. This suggests that the stability of the modes can be partially attributed to their low k-values, as explained earlier. However, low k-modes can also be trapped. If the 213 s doublet in ZZ Ceti consists of trapped modes, then indeed our subsequent measurement of the $\dot{P}$ will reflect the stability of the trapping mechanism, which is related to the cooling rate. Presently, we have only an upper limit for $\dot{P}$, and we cannot conclude whether these modes are trapped.

We expect the uncertainties in measuring $\dot{P}$ to decrease as the square of the time base.[47] This implies that if we continue acquiring data with the same telescopes and PMT photometers, we would need 95 years of data to reduce the uncertainties by a factor of 10. However, with our new higher quantum efficiency CCD photometer, we get the same signal-to-noise ratio as the PMT photometer on a 6 m telescope (Nather & Mukadam 2003). If we acquire longer data sets with CCD photometers, use larger telescopes, or make a combination of both every few years, then we could achieve a significant reduction in the uncertainties in a shorter time span.

6.2. *Summary of Results for the* 274 s *Doublet*

The implied $\dot{P}$ from the $O-C$ diagram for the 274 s doublet is 100 times larger than the $\dot{P}$ for the 213 s doublet. Long-term limits from the direct method in § 4.1 indicate that $|\dot{P}| \sim 3 \times 10^{-12}$ s s^{-1} for the 274 s doublet. The minimum dispersion in the $O-C$ diagram, which does not fit a parabola, allows us to set a lower limit $\Delta P/\Delta t \approx 10^{-13}$ s s^{-1} for the long-term behavior. We do not know yet what this period variation entails, but we know that it is not consistent with cooling, as cooling is the slowest of all possible timescales. For both modes of the 274 s doublet, we could never achieve a clear minimization of phase dispersion. The uncertainties in phase are larger for the 274 s doublet as it has a lower amplitude compared with the 213 s doublet, but not low enough to explain away the discrepancies. We obtain an $O-C$ diagram with ambiguous cycle counts, and all the points do not lie on a parabola within the uncertainties. This suggests that $\dot{P}$ for the 274 s doublet is not constant and perhaps $\ddot{P}$ and/or higher order terms are significant.

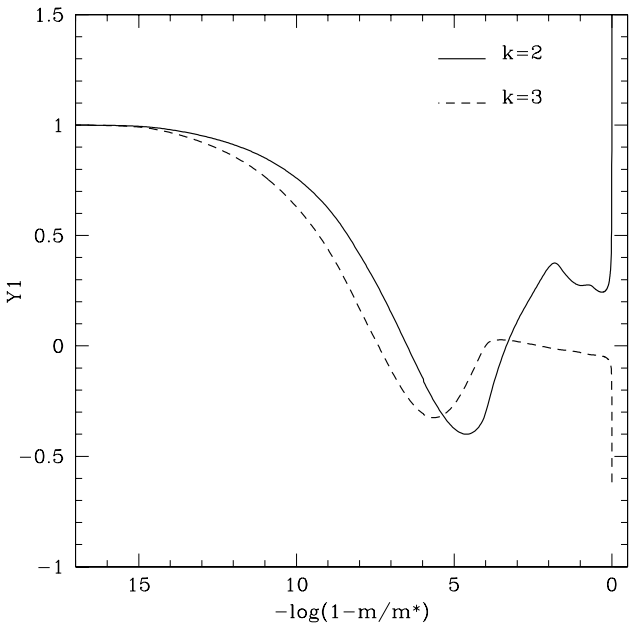

FIG. 5.—Radial perturbation ($Y_1 = \delta r/r$) for the best model of ZZ Ceti calculated by Bradley (1998), showing eigenfunction for the $k = 3$ mode. This mode corresponds to the 274 s periodicities and has negligible amplitude from the center [$\log(1 - M/M_*) = 0$] to the envelope [$\log(1 - M/M_*) \leq 4$] compared with the $k = 2$ mode, which corresponds to the 213 s periodicities.

We should remind ourselves that the two doublets sample different regions of the star. Bradley (1998) calculated nonradial perturbations for the best model of ZZ Ceti, given by $T_{\rm eff} = 12,420$ K, $M_* = 0.54$ $M_\odot$, hydrogen layer mass $M_{\rm H} = 0.00015 M_*$, helium layer mass $M_{\rm He} = 0.015 M_*$, and ML3 convection. The eigenfunctions for the $l = 1$, $k = 3$ mode or the 274 s doublet show negligible amplitude near the center of the star compared with the $l = 1$, $k = 2$ mode, which corresponds to the 213 s doublet. This is clearly indicated in Figure 5. It is possible that the 274 s doublet has a larger $\dot{P}$ because it samples regions of the star that could be undergoing changes on timescales shorter than the evolutionary timescale.

An avoided crossing, described below, represents another explanation for the 274 s doublet. Wood & Winget (1988) carried out pulsation calculations in the quasi-adiabatic Cowling approximation for $l = 2$, $k = 1, \ldots, 16$. They evolved their models from 13,000 to 11,000 K across the DAV instability strip. Figures 1 and 2 in their paper clearly show $k = 6$ as the trapped mode at the hot end of the sequence. As the star cools, the kinetic energies of the $k = 5$ and $k = 6$ modes pull closer together. At this point, the physical properties of the two modes become nearly identical, and they become indistinguishable from the driving mechanism. As the models continue to evolve, $k = 5$ becomes the new trapped mode. These modes have effectively interchanged their nature, and this phenomenon is known as an avoided crossing (Aizenman, Smeyers, & Weigert 1977; Christensen-Dalsgaard 1981). Of the 16

[47] Kepler et al. 2000 find that the uncertainties decrease linearly with time for G117-B15A. However, this may possibly be associated with the observed 1.8 s scatter (Kepler et al. 2000 and references therein).

modes, four were computed to undergo such an avoided crossing, i.e., one of every four modes may be expected to undergo an avoided crossing.

Stable modes can become unstable during an avoided crossing (Wood & Winget 1988; Montgomery & Winget 1999), as explained in § 6.2. In other words, if we were monitoring the $\dot{P}$ for any of these modes, we would observe a rapid change during the crossover; i.e., the $\ddot{P}$ term would be important. Montgomery & Winget (1999) have done the most detailed calculation to date, showing how the g-mode periods evolve as the crystallized mass fraction is slowly increased. Their results, plotted in Figure 9 of their paper, clearly show many kinks or avoided crossings. Wood & Winget (1988), as well as Bradley & Winget (1991), saw similar behavior in their evolutionary calculations, when they included H and He layers in their models. The 274 s doublet in ZZ Ceti could be undergoing an avoided crossing, but this issue needs to be investigated more thoroughly.

Possibly the 274 s doublet is undergoing other short-term phase variations,[48] perhaps associated with the presence of nearby undetected modes, that have been successful in swamping out the cooling effect. Variations in $\dot{P}$ at short timescales on the order of a few months to a few years, superposed on the secular cooling (Dziembowski & Koester 1981), that average out over 30 years could explain the partial stability that we see. However, such short-term phase variations could render a parabolic fit to the $O-C$ diagram difficult, thus swamping out changes in period due to cooling. We cannot place any limits on the short-term behavior, as we have large gaps between data sets.

We hope to attempt to unravel this mystery by obtaining additional multisite and extensive single-site data for an additional 6 or 7 years. As both the 213 s doublet in ZZ Ceti and the 215 s mode in G117-B15A show a similar $\dot{P}$, it would be worthwhile to find out whether the 270 s mode in G117-B15A behaves like the 274 s doublet in ZZ Ceti.

7. ADDITIONAL PULSATION MODES

Our FTs from the various seasonal data sets showed additional pulsations around 187.27, 318.08, and 333.65 s. Observations of ZZ Ceti with the 3.6 m CFHT in 1991 clearly revealed these modes, though the result remained unpublished till now. An FT of the 1991 data set, after prewhitening or removing the two doublets, is shown in Figure 6. We can clearly see the new modes along with the residual amplitude of the two doublets left behind in the prewhitening process.[49] Table 5 gives our best estimates for the periods and amplitudes for the various years of observation. The amplitudes of these modes are small enough that determining their precise frequencies is difficult.

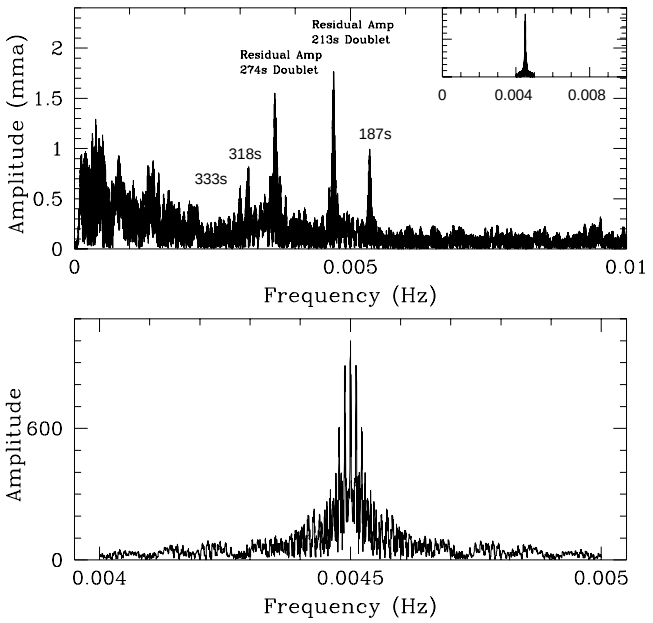

FIG. 6.—*Top*: Prewhitened FT of the 1991 data set, clearly showing the additional modes 187, 318, and 333 s. The doublets were not prewhitened completely, and some residual amplitude is left behind. *Bottom*: Window pattern.

With the discovery of three additional modes in ZZ Ceti, we now have five modes with different l and k values. Bradley (1998) pointed out various feasible mode identifications for the pulsation periods observed in ZZ Ceti (see his § 5.6). The confirmation of the 187, 318, and 333 s modes suggest that the 213 and 274 s doublets (caused by

[48] We have searched for variations in phase at timescales from a few days to a month or so and found none.

[49] Prewhitening of individual seasons leaves behind some residual amplitude, which can be interpreted as a third frequency with an amplitude ≤ 2 mma, implying that the 213 and 274 s modes are actually triplets and not doublets. We prewhitened various seasons with the two known periods at 213 and 274 s and then attempted to determine the third frequency by using a nonlinear least-squares fit to the residual amplitude. We obtained different frequencies with differing amplitudes from the various seasons. This implies that from the quality of data in hand we can neither conclude that we have a triplet nor rule it out. To resolve this issue, we need very high signal-to-noise data for at least three seasons, which clearly shows evidence of the triplet even without prewhitening; frequencies determined from prewhitening alone are not reliable. Other causes of the residual amplitude could include timing uncertainties of individual runs in a season and/or amplitude changes.

TABLE 5
PERIOD AND AMPLITUDE MEASUREMENTS FOR THE ADDITIONAL PULSATION MODES

Season	Period (s)	Amplitude (mma)	Period (s)	Amplitude (mma)	Period (s)	Amplitude (mma)
1991	333.636 ± 0.015	0.64 ± 0.08	318.049 ± 0.011	0.85 ± 0.08	187.272 ± 0.003	0.93 ± 0.08
1993	...	...	...	...	187.267 ± 0.002	0.85 ± 0.13
1999 Sep–Oct	333.642 ± 0.004	0.51 ± 0.16	318.075 ± 0.002	0.93 ± 0.16	...	...
1999 Nov	333.634 ± 0.010	1.31 ± 0.17	318.082 ± 0.015	0.82 ± 0.17	...	...
2000	333.668 ± 0.004	0.67 ± 0.15	318.080 ± 0.003	0.67 ± 0.15	...	...
2001	333.639 ± 0.001	1.03 ± 0.13	318.074 ± 0.001	1.10 ± 0.13	187.286 ± 0.001	0.43 ± 0.12

rotational splitting) are probably $l = 1$, $k = 2$ and $l = 1$, $k = 3$ modes, respectively (Bradley 1998). He shows that models with this mode identification have periods that best match the newly identified modes. The three new modes are most likely $l = 2$ modes with $k = 4$, $k = 8$, and $k = 9$ (Bradley 1998). This mode identification also suggests that ZZ Ceti has a mass near 0.54 $M_\odot$, a 65%–80% oxygen core, a hydrogen layer mass of $0.00015M_*$, and a helium layer mass near $0.015M_*$ (Bradley 1998). Bergeron et al. (1995) determined an effective temperature $T_{\rm eff} = 11,990$ K, $\log g = 7.97$, and a mass of 0.59 $M_\odot$ from high signal-to-noise optical spectrophotometry data on ZZ Ceti by using new model atmospheres.

8. IMPLICATIONS AND APPLICATIONS

White dwarf cosmochronometry.—Some of the theoretical uncertainty in using white dwarfs as chronometers to constrain the age of the Galactic disk (e.g., Winget et al. 1987) and the halo (e.g., Hansen et al. 2002) can be reduced by calibrating the white dwarf cooling curve. This involves empirical measurements of the cooling rates of white dwarfs at different temperatures. Our upper limit on the rate of cooling of ZZ Ceti already constrains theoretical evolutionary models. Our constraint along with the $\dot{P}$ measurements for PG 1159-035 (Costa et al. 1999) and G117-B15A (Kepler et al. 2000) helps in calibrating the white dwarf cooling curve.

Core composition.—The rate of cooling of a white dwarf depends mainly on core composition and stellar mass. For a given core mass, a larger mean atomic weight will correspond to fewer nuclei with smaller heat capacity, resulting in more rapid cooling. By constraining the rate of cooling for ZZ Ceti and comparing it with theoretical evolutionary models, we effectively limit the mean atomic weight of the core. Bradley et al. (1992) obtained theoretical $\dot{P}$ values around $(5–7) \times 10^{-15}$ s s^{-1} from detailed calculations for untrapped modes in oxygen core 0.5 $M_\odot$ models with periods close to 215 s. Panei, Althaus, & Benvenuto (2000) find that models with a pure iron core cool faster than their carbon-oxygen counterparts up to a factor of 5. This implies that our current limit of 5.5×10^{-15} s s^{-1} indicates a carbon-oxygen core and eliminates substantially heavier cores, as they would produce a faster rate of period change than observed.

Stable clock.—ZZ Ceti is the second most stable optical clock known. Moreover, the drift in this clock is unidirectional and predictable as it is caused by cooling of the star. This characteristic makes clocks such as ZZ Ceti and G117-B15A comparable to atomic clocks and better than most pulsars. Atomic clocks demonstrate an uncertainty in phase that is best described as a random walk, while many pulsars are known to have an inherent noise level on the order of 10^{-14} s s^{-1} (Kaspi, Taylor, & Ryba 1994), in addition to star quakes that cause glitches. The millisecond pulsar PSR B1885+09, however, is more stable than both ZZ Ceti and G117-B15A. It has a period of 5.36 ms and a measured $\dot{P} = 1.78363 \times 10^{-20}$ s s^{-1} (Kaspi et al. 1994), which implies that the stability timescale is $\tau_s \approx 9.5$ Gyr. We compute τ_s longer than 3.0 and 1.2 Gyr for G117-B15A and ZZ Ceti, respectively.

We note that G117-B15A and ZZ Ceti are stable enough to act as a reference for the atomic clock system that underpins the GPS network. National Institute of Standards and Technology (NIST) claims an uncertainty of 2×10^{-15} for NIST-F1 (Bergquist, Jefferts, & Wineland 2001), the cesium fountain atomic clock, which defines the most accurate primary time and frequency standard to date. We compute $\tau_s = 15.1$ hr for the clock.

Orbital companion.—A stable clock with an orbital companion will revolve around the center of mass of the system, thus changing the light travel time of the pulse maxima. The variable period resulting from the orbital motion of the clock will cause a $\dot{P}_{\rm orb}$ (Kepler et al. 1991), the amplitude of which is the orbital light travel time.

Detection of an orbital companion around a pulsating white dwarf depends on the following parameters: the mass m of the companion and the inclination angle i ($\dot{P}_{\rm orb} \propto m \sin i$), its distance a from the white dwarf ($\dot{P}_{\rm orb} \propto 1/a^2$), and the orbital period T, all of which are not independent. The first two criteria are easy to understand; if the companion is not massive or far away from the white dwarf, then its gravitational influence may not be detectable. The third criterion is more subtle. When we observe pulsating white dwarfs, we do not directly measure $\dot{P}$. We infer a $\dot{P}$ by comparing our measurements of the phases with what we expect for a constant period, i.e., by using the $O-C$ technique. The phase difference, $O-C$, increases because of an orbital companion for half an orbital period, after which it must start decreasing. At the end of an orbital period, the $O-C$ must reflect a change from cooling alone. So, the phase variation amplitude in the $O-C$ diagram depends not only on the magnitude of $\dot{P}_{\rm orb}$ but also on the time for which the phase change was allowed to accumulate, i.e., $T/2$.

With this technique, it is easier to detect companions with large orbital periods, though that will necessarily require long-term observations. The phase changes are cumulative, and so in the limit of slow changes (long orbital periods) our limits improve as time-square goes by. Nearby planets with shorter orbital periods may be detected by decreasing the uncertainties on individual phase measurements.

The following examples demonstrate the sensitivity of this technique. An Earthlike planet orbiting ZZ Ceti at a distance of 1 AU will result in $\dot{P}_{\rm orb}^{\rm Earth} = 12.5 \times 10^{-15}$ s s^{-1} and a phase variation amplitude of a few milliseconds. Detection on Earth requires greater timing accuracy than current observations of ZZ Ceti and G117-B15A, even though $\dot{P}_{\rm orb}$ is more than twice as large as the evolutionary $\dot{P}$. Jupiter ($M = 318$ $M_\oplus$) at 5.2 AU will result in $\dot{P}_{\rm orb} = 1.5 \times 10^{-13}$ s s^{-1} with an amplitude of 3–4 s. We can use our current detection limit of 1 s, constrained by our timing accuracy, to limit the mass and/or distance of any planetary companions around ZZ Ceti. Setting $\dot{P}_{\rm orb} = 5.5 \times 10^{-15}$ s s^{-1}, we are able to rule out planetary companions of masses $M \geq 38$ $M_\oplus$ at distances $a \leq 9$ AU from ZZ Ceti.

Asteroseismology.—With the discovery of three additional modes in ZZ Ceti, we now have five known independent modes. This helps us in mode identification and leads to constraining the stellar structure through asteroseismology. It will also assist in the work on ensemble asteroseismology of DAVs (Kleinman, Kawaler, & Bischoff 2000). Metcalfe, Nather, & Winget (2000) have applied an optimization method utilizing a genetic algorithm for fitting white dwarf pulsation models to asteroseismological data. For the success of this technique, they require at least seven or eight observed modes. With the additional modes found in ZZ Ceti, coupled to the fact that it shows low-amplitude

sinusoidal variations, it becomes an attractive candidate for such work.

9. CONCLUSION

We obtained extensive multi- and single-site data on ZZ Ceti, thereby increasing the existing time span of data by 8 years, to a total of 31 years. We applied the direct method on resolved seasons to help us rule out large changes in period over time. Confident of our limits from the direct method, we then searched in a narrow grid of solution space with two of the more sensitive techniques, the $O - C$ diagram and the nonlinear least-squares approach. We arrived at the best upper limit for the rate of period change for ZZ Ceti, $\dot{P} \leq (5.5 \pm 1.9) \times 10^{-15}$ s s^{-1}. This usefully constrains secular cooling, demonstrating an evolutionary timescale or stability timescale $| P/\dot{P} | \geq 1.2$ Gyr. We obtain a stability timescale $\tau_s \geq 0.9$ Gyr at the 1 σ level and $\tau_s \geq 0.6$ Gyr at the 3 σ level. Theoretical models suggest that the 213 s doublet in ZZ Ceti should show a $\dot{P}$ value in the range of $(2\text{–}6) \times 10^{-15}$ s s^{-1} (e.g., Bradley et al. 1992; Bradley 1996).

Limits from the direct method and the minimum dispersion in the $O - C$ diagram, which does not fit a parabola, allow us to set a lower limit $\Delta P/\Delta t \approx 10^{-13}$ s s^{-1} on the long-term behavior of the 274 s doublet. The implied limit does not reflect cooling, as cooling causes the slowest change in period with time, and is constrained by the 213 s doublet to be on the order of 10^{-15} s s^{-1}. The 274 s doublet, which samples a different region of the star than the 213 s doublet, may be undergoing an avoided crossing or other short-term phase variations, perhaps associated with the presence of nearby undetected modes. To investigate this issue, we need extensive single and multisite data for an additional 6–7 years.

We acknowledge and thank NSF for grant AST 98-76730, NASA for grant NAG 5-9321, and STScI for grant GO-08254. We thank the NSF International Travel Grant for support to attend the Sixth WET Workshop in June in Naples, where this work was presented. We also acknowledge the Spanish grants PB97-1435-C02-02 and AYA2000-1691, as well as the Polish grant KBN 5-P03D-012-20, for their financial support. We thank the referee, Detlev Koester, for his helpful comments and suggestions that made this paper a better manuscript.

REFERENCES

Aizenman, M., Smeyers, P., & Weigert, A. 1977, A&A, 58, 41
Benvenuto, O. G., Córsico, A. H., Althaus, L. G., & Serenelli, A. M. 2002, MNRAS, 335, 480
Bergeron, P., Wesemael, F., Lamontagne, R., Fontaine, G., Saffer, R. A., & Allard, N. F. 1995, ApJ, 449, 258
Bergquist, J. C., Jefferts, S. R., & Wineland, D. J. 2001, Phys. Today, 2001 (March), 37
Bradley, P. A. 1993, Ph.D. thesis, Univ. Texas Austin
———. 1996, ApJ, 468, 350
———. 1998, ApJS, 116, 307
Bradley, P. A., & Winget, D. E. 1991, ApJS, 75, 463
Bradley, P. A., Winget, D. E., & Wood, M. A. 1992, ApJ, 391, L33
Brassard, P., Fontaine, G., Wesemael, F., & Hansen, C. J. 1992, ApJS, 80, 369
Christensen-Dalsgaard, J. 1981, MNRAS, 194, 229
Costa, J. E. S., Kepler, S. O., & Winget, D. E. 1999, ApJ, 522, 973
Duncan, M. J., & Lissauer, J. J. 1998, Icarus, 134, 303
Dziembowski, W., & Koester, D. 1981, A&A, 97, 16
Fontaine, G., Bergeron, P., Lacombe, P., Lamontagne, R., & Talon, A. 1985, AJ, 90, 1094
Hansen, B. M. S., et al. 2002, ApJ, 574, L155
Harrington, R. S., & Dahn, C. C. 1980, AJ, 85, 454
Kanaan, A., O'Donoghue, D., Kleinman, S. J., Krzesinski, J., Koester, D., & Dreizler, S. 2000, Baltic Astron., 9, 387
Kaspi, V. M., Taylor, J. H., & Ryba, M. F. 1994, ApJ, 428, 713
Kepler, S. O. 1993, Baltic Astron., 2, 515
Kepler, S. O., Mukadam, A., Winget, D. E., Nather, R. E., Metcalfe, T. S., Reed, M. D., Kawaler, S. D., & Bradley, P. A. 2000, ApJ, 534, L185
Kepler, S. O., Robinson, E. L., Nather, R. E., & McGraw, J. T. 1982, ApJ, 254, 676
Kepler, S. O., et al. 1990, ApJ, 357, 204
———. 1991, ApJ, 378, L45
Kleinman, S. J., Kawaler, S. D., & Bischoff, A. 2000, in ASP Conf. Ser. 203, The Impact of Large-Scale Surveys on Pulsating Star Research, ed. L. Szabados & D. W. Kurtz (San Francisco: ASP), 515
Kleinman, S. J., Nather, R. E., & Phillips, T. 1996, PASP, 108, 356
Kleinman, S. J., et al. 1998, ApJ, 495, 424
Mestel, L. 1952, MNRAS, 112, 583
Metcalfe, T. S., Nather, R. E., & Winget, D. E. 2000, ApJ, 545, 974
Montgomery, M. H. 1998, Ph.D. thesis, Univ. Texas Austin
Montgomery, M. H., & Winget, D. E. 1999, ApJ, 526, 976
Mukadam, A. S. 2000, Master's thesis, Univ. Texas Austin
Mukadam, A. S., Winget, D. E., & Kepler, S. O. 2001, in ASP Conf. Ser. 226, 12th European Workshop on White Dwarfs, ed. L. Provencal, H. L. Shipman, J. MacDonald, & S. Goodchild (San Francisco: ASP), 337
Mukadam, A. S., et al. 2003, Baltic Astron., 12, 71
Nather, R. E., & Mukadam, A. S. 2003, preprint (astro-ph/0306022)
Nather, R. E., Winget, D. E., Clemens, J. C., Hansen, C. J., & Hine, B. P. 1990, ApJ, 361, 309
Nitta, A., et al. 1999, in ASP Conf. Ser. 169, 11th European Workshop on White Dwarfs, ed. J. E. Solheim & E. G. Meistas (San Francisco: ASP), 144
Pajdosz, G. 1995, A&A, 295, L17
Panei, J. A., Althaus, L. G., & Benvenuto, O. G. 2000, MNRAS, 312, 531
Robinson, E. L. 1979, IAU Colloq. 53, White Dwarfs and Variable Degenerate Stars, ed. H. M. Van Horn & V. Weidemann (Rochester: Univ. Rochester Press), 343
Robinson, E. L., Kepler, S. O., & Nather, R. E. 1982, ApJ, 259, 219
Schmidt, G. D., & Grauer, A. D. 1997, ApJ, 488, 827
Schwarzenberg-Czerny, A. 1991, MNRAS, 253, 198
———. 1999, ApJ, 516, 315
Standish, E. M. 1998, A&A, 336, 381
Stover, R. J., Nather, R. E., Robinson, E. L., Hesser, J. E., & Lasker, B. M. 1980, ApJ, 240, 865
Tomaney, A. B. 1987, in IAU Colloq. 95, Second Conference on Faint Blue Stars, ed. A. G. Davis Philip, D. S. Hayes, & J. W. Liebert (Dordrecht: Reidel), 673
Van Horn, H. M. 1971, in IAU Symp. 42, White Dwarfs, ed. W. J. Luyten (Dordrecht: Reidel), 97
Vassiliadis, E., & Wood, P. R. 1993, ApJ, 413, 641
Winget, D. E. 1998, J. Phys. Condensed Matter, 10, 11247
Winget, D. E., Hansen, C. J., & Van Horn, H. M. 1983, Nature, 303, 781
Winget, D. E., Robinson, E. L., Nather, R. E., Kepler, S. O., & O'Donoghue, D. 1985, ApJ, 292, 606
Winget, D. E., Van Horn, H. M., & Hansen, C. J. 1981, ApJ, 245, L33
Winget, D. E., et al. 1987, ApJ, 315, L77
Wood, M. A., & Winget D. E. 1988, in Proc. Multimode Stellar Pulsations Workshop, ed. G. Kovacs, L. Szabados, & B. Szeidl (Budapest: Konkoly Obs.), 199